

# Alternative methods for measurement of the global polarization of $\Lambda$ hyperons<sup>\*</sup>

Irfan Siddique<sup>1</sup> Zuo-tang Liang(梁作堂)<sup>2</sup> Michael Annan Lisa<sup>3</sup> Qun Wang(王群)<sup>1;1)</sup> Zhang-bu Xu(许长补)<sup>2,4</sup>

<sup>1</sup> Department of Modern Physics, University of Science and Technology of China, Hefei, Anhui 230026, China

<sup>2</sup> School of Physics & Key Laboratory of Particle Physics and Particle Irradiation (MOE)

<sup>3</sup> Physics Department, The Ohio State University, Columbus, Ohio 43210, USA

<sup>4</sup> Physics Department, Brookhaven National Laboratory, Upton, New York 11973-5000, USA

**Abstract:** We propose alternative methods for measurement of the global polarization of  $\Lambda$  hyperons. These methods involve event averages of proton and  $\Lambda$  momenta in the laboratory frame. We carry out simulations using these methods and show that all of them work equally well in obtaining the global polarization of  $\Lambda$  hyperons.

**Keywords:** heavy ion collisions, global polarization, collective flow

**PACS:** 25.75.-q **DOI:** 10.1088/1674-1137/43/1/014103

## 1 Introduction

It is well-known that rotation and polarization are inherently correlated: the rotation of an uncharged object can lead to spontaneous magnetization and polarization, and vice versa [1, 2]. We expect that the same phenomena exist in heavy ion collisions. It is straightforward to estimate the huge global angular momenta that are generated in non-central heavy ion collisions at high energies [3–8]. How such huge global angular momenta are converted to particle polarization in the hot and dense matter, and how can the global polarization be measured, are two core questions to be answered. Several theoretical models are available that address the first question, e.g. the microscopic spin-orbital coupling model [3, 4, 8, 9], the statistical-hydro model [10–13] and the kinetic model with Wigner functions [14–17], see Ref. [18] for a recent review. As for the second question, the weak decay property of  $\Lambda$  hyperons can be used for measurement of the global polarization [3, 4]: the parity-breaking weak decay of  $\Lambda$  into a proton and a pion is self-analyzing since the daughter proton is emitted preferentially along the spin of the  $\Lambda$  in its rest frame [5, 19]. The global polarization of a vector meson can be measured using the angular distribution of its decay products, which is related to the elements of its spin density matrix [4].

Recently, the global polarization of  $\Lambda$  and  $\bar{\Lambda}$  hyperons was measured for collision energies below 62.4 GeV [20, 21]. The average values of the global polarization for  $\Lambda$  and  $\bar{\Lambda}$  are  $\mathcal{P}_\Lambda = (1.08 \pm 0.15)\%$  and  $\mathcal{P}_{\bar{\Lambda}} = (1.38 \pm 0.30)\%$ .

The polarization of  $\bar{\Lambda}$  is somewhat larger than that of  $\Lambda$ , and is thought to be caused by a negative (positive) magnetic moment of  $\Lambda(\bar{\Lambda})$  in magnetic fields. However, the difference is negligible, it is well within the error bars, and the magnetic fields extracted from the data are consistent with zero. The global polarization of  $\Lambda$  and  $\bar{\Lambda}$  decreases with collision energy. This is due to the fact that Bjorken scaling works better at higher energies. From the data one can estimate the local vorticity:  $\omega = (9 \pm 1) \times 10^{21} \text{ s}^{-1}$ , implying that the matter created in ultra-relativistic heavy ion collisions is the most vortical fluid that exists in nature. The vorticity field of the quark gluon plasma has been studied by many authors using a variety of methods including hydrodynamical models [22–24] and transport models [25, 26]. The global polarization of  $\Lambda$  and  $\bar{\Lambda}$  has also been calculated by hydrodynamical models [27, 28], the transport model [29] and the chiral kinetic model [30].

The method used in the STAR experiment is by event averaging of  $\sin(\phi_p^* - \psi_{\text{RP}})$ , where  $\phi_p^*$  and  $\psi_{\text{RP}}$  are the azimuthal angles, in the  $\Lambda$  rest frame, of the proton momentum and of the reaction plane, respectively [20, 21]. The orientation of the reaction plane cannot be directly measured; it is derived from the event plane, itself determined from the direct flow. Therefore, a reaction plane resolution factor was introduced to account for the finite resolution of the reaction plane as given by the detector [20, 21].

In this paper, we propose alternative methods for measurement of the global polarization of  $\Lambda$  and  $\bar{\Lambda}$  hy-

Received 25 August 2018, Published online 20 November 2018

<sup>\*</sup> IS and QW are Supported in part by the Major State Basic Research Development Program (MSBRD) in China (2015CB856902, 2014CB845402) and the National Natural Science Foundation of China (NSFC) (11535012)

1) E-mail: qunwang@ustc.edu.cn

©2019 Chinese Physical Society and the Institute of High Energy Physics of the Chinese Academy of Sciences and the Institute of Modern Physics of the Chinese Academy of Sciences and IOP Publishing Ltd

perons based on the Lorentz transformation. The advantage of these methods is that all event averages are taken using momenta in the lab frame instead of the  $\Lambda$  rest frame. We compare these methods by simulations and show that all of them work equally well in obtaining the global polarization of  $\Lambda$  hyperons.

## 2 Hyperon weak decay and polarization

The polarization of the  $\Lambda$  (and  $\bar{\Lambda}$ ) hyperons can be measured by its parity-breaking weak decay  $\Lambda \rightarrow p + \pi^-$ . The daughter proton is emitted preferentially along the  $\Lambda$  polarization in its rest frame. The angular distribution of the daughter proton reads

$$\frac{dN}{d\Omega^*} = \frac{1}{4\pi} \left( 1 + \alpha_H \mathcal{P}_\Lambda \frac{\mathbf{n}^* \cdot \mathbf{p}^*}{|\mathbf{p}^*|} \right), \quad (1)$$

where  $\alpha_H$  is the hyperon decay parameter,  $\mathcal{P}_\Lambda$  is the  $\Lambda$  global polarization;  $\mathbf{n}^*$ ,  $\mathbf{p}^*$  and  $\Omega^*$  are the  $\Lambda$  polarization, the proton momentum and its solid angle in the rest frame of the hyperon, respectively, labeled by the superscript '\*'. We note that Eq. (1) is Lorentz invariant by observing

$$\begin{aligned} \mathbf{n}^* \cdot \mathbf{p}^* &= -n_\mu p^\mu = -n \cdot p, \\ E_p^* &= \frac{1}{2m_\Lambda} (m_\Lambda^2 + m_p^2 - m_\pi^2), \\ |\mathbf{p}^*| &= \frac{1}{2m_\Lambda} \sqrt{[m_\Lambda^2 - (m_p - m_\pi)^2][m_\Lambda^2 - (m_p + m_\pi)^2]}, \end{aligned} \quad (2)$$

where  $p^\mu$  and  $p_\Lambda^\mu$  are the four-momenta of the proton and the hyperon in any frame, respectively, and  $n^\mu$  is the space-like four-vector of the hyperon polarization in a general frame. We now focus on the lab frame and the hyperon rest frame. We use  $p^\mu$ ,  $p_\Lambda^\mu$  and  $n^\mu$  to label quantities in the lab frame; all quantities with the superscript '\* are in the hyperon rest frame. The Lorentz transformation of the  $\Lambda$  polarization is,

$$n^\mu = \Lambda_\nu^\mu(-\mathbf{v}_\Lambda) n^{*\nu}, \quad (3)$$

where  $\Lambda_\nu^\mu(-\mathbf{v}_\Lambda)$  is the Lorentz transformation with  $\mathbf{v}_\Lambda = \mathbf{p}_\Lambda/E_\Lambda$ . The  $\Lambda$  polarization in the rest frame  $n^{*\nu}$  has the form  $n^{*\mu} = (0, \mathbf{n}^*)$  where  $\mathbf{n}^*$  is the three-vector of the polarization with  $|\mathbf{n}^*|^2 < 1$ . From Eq. (3) we have

$$n^\mu = (n_0, \mathbf{n}) = \left( \frac{\mathbf{n}^* \cdot \mathbf{p}_\Lambda}{m_\Lambda}, \mathbf{n}^* + \frac{(\mathbf{n}^* \cdot \mathbf{p}_\Lambda) \mathbf{p}_\Lambda}{m_\Lambda(m_\Lambda + E_\Lambda)} \right). \quad (4)$$

We can also express  $n^{*\mu}$  in terms of  $n^\mu$ ,

$$n^{*\mu} = \Lambda_\nu^\mu(\mathbf{v}_\Lambda) n^\nu, \quad (5)$$

or explicitly,

$$n^{*\mu} = (0, \mathbf{n}^*) = \left( 0, \mathbf{n} - \frac{\mathbf{p}_\Lambda (\mathbf{n} \cdot \mathbf{p}_\Lambda)}{E_\Lambda (E_\Lambda + m_\Lambda)} \right). \quad (6)$$

The polarization four-vector of a particle is always orthogonal to its four-momentum,  $n \cdot p_\Lambda = n^0 E_\Lambda - \mathbf{n} \cdot \mathbf{p}_\Lambda = 0$ ,

so we can express  $n^0$  in term of  $\mathbf{n}$ ,  $n^0 = \mathbf{n} \cdot \mathbf{v}_\Lambda$ . One can verify that  $n^\mu$  in Eq. (4) satisfies  $n^0 = \mathbf{n} \cdot \mathbf{v}_\Lambda$ . From  $(n^0)^2 - |\mathbf{n}|^2 = -|\mathbf{n}^*|^2$  and  $n^0 = \mathbf{n} \cdot \mathbf{v}_\Lambda$ , we can solve for  $|\mathbf{n}|^2$  giving

$$|\mathbf{n}|^2 = \frac{|\mathbf{n}^*|^2}{1 - |\mathbf{v}_\Lambda|^2 (\hat{\mathbf{n}} \cdot \hat{\mathbf{v}}_\Lambda)^2}. \quad (7)$$

We see that when  $|\mathbf{v}_\Lambda|^2 (\hat{\mathbf{n}} \cdot \hat{\mathbf{v}}_\Lambda)^2 \rightarrow 1$ ,  $|\mathbf{n}|^2 \rightarrow \infty$ , i.e.  $|\mathbf{n}|^2$  is not bounded. In case of transverse polarization, i.e.  $\hat{\mathbf{n}} \cdot \hat{\mathbf{v}}_\Lambda = 0$ , we have  $|\mathbf{n}|^2 = |\mathbf{n}^*|^2 < 1$ .

In the lab frame, a 3-dimensional vector (e.g. impact parameter, global angular momentum, beam direction) can be written as  $\mathbf{a} = a_x \mathbf{e}_x + a_y \mathbf{e}_y + a_z \mathbf{e}_z$ , where  $(\mathbf{e}_x, \mathbf{e}_y, \mathbf{e}_z)$  are the three basis directions.

## 3 STAR method for measurement of the $\Lambda$ hyperon polarization

In this section we describe briefly the method used in the STAR experiment for measurement of the  $\Lambda$  hyperon polarization [21]. From Eq. (13), we can determine the  $\Lambda$  polarization in its rest frame by taking the event average of the direction of the proton momentum  $\hat{\mathbf{p}}^*$ . We then make a projection onto the direction of the global angular momentum  $\mathbf{e}_L$ ,

$$\mathcal{P}_\Lambda = \frac{3}{\alpha_H} \langle \hat{\mathbf{p}}^* \cdot \mathbf{e}_L \rangle_{ev} = \frac{3}{\alpha_H} \langle \cos \theta^* \rangle_{ev} \quad (8)$$

where  $\theta^*$  is the angle, in the  $\Lambda$  rest frame, between the proton momentum and the global angular momentum corresponding to the reaction plane. We have the following relation

$$\cos \theta^* = \sin \theta_p^* \sin(\phi_p^* - \psi_{RP}), \quad (9)$$

where  $\theta_p^*$  and  $\phi_p^*$  are the polar and azimuthal angles of  $\hat{\mathbf{p}}^*$ , respectively, and  $\psi_{RP}$  is the azimuthal angle of the reaction plane. We integrate over  $\theta_p^*$  in Eq. (1) to obtain

$$\frac{dN}{d\phi_p^*} = \int_0^\pi d\theta_p^* \sin \theta_p^* \frac{dN}{d\Omega^*} = \frac{1}{2\pi} + \frac{1}{8} \alpha_H \mathcal{P}_\Lambda \sin(\phi_p^* - \psi_{RP}), \quad (10)$$

which gives the polarization in terms of the azimuthal angle of the daughter proton,

$$\mathcal{P}_\Lambda = \frac{8}{\pi \alpha_H} \langle \sin(\phi_p^* - \psi_{RP}) \rangle_{ev}, \quad (11)$$

with

$$\langle \sin(\phi_p^* - \psi_{RP}) \rangle_{ev} = \int_0^{2\pi} d\phi_p^* \frac{dN}{d\phi_p^*} \sin(\phi_p^* - \psi_{RP}). \quad (12)$$

In the STAR experiment, the azimuthal angle of the reaction plane cannot be directly measured. It is determined from the measurement of the event plane given by the direct flow. This introduces a reaction plane resolution factor in the denominator of Eq. (11),

$R_{\text{EP}}^{(1)} = \left\langle \cos(\psi_{\text{RP}} - \psi_{\text{EP}}^{(1)}) \right\rangle_{\text{ev}}$ , where  $\psi_{\text{EP}}^{(1)}$  is the azimuthal angle of the event plane determined by the direct flow.

#### 4 Alternative methods

In this section, we introduce alternative methods for measurement of the  $\Lambda$  hyperon polarization. The advantage of these methods is that the polarization can be measured using the proton momentum in the lab frame.

We start with the formula for the  $\Lambda$  polarization vector in its rest frame,

$$\vec{\mathcal{P}}_{\Lambda} = \frac{3}{\alpha_H} \langle \hat{\mathbf{p}}^* \rangle_{\text{ev}}. \quad (13)$$

We can project the above onto the direction of the global polarization, which we assume to be along the  $y$ -axis, see Fig. (1).

We now try to evaluate  $\langle \hat{\mathbf{p}}^* \rangle_{\text{ev}}$ . To this end, we use the following Lorentz transformation of the proton momentum,

$$\mathbf{p} = \mathbf{p}^* + \frac{\mathbf{p}_{\Lambda}(\mathbf{p}^* \cdot \mathbf{p}_{\Lambda})}{m_{\Lambda}(E_{\Lambda} + m_{\Lambda})} + \frac{E_{\text{p}}^*}{m_{\Lambda}} \mathbf{p}_{\Lambda}, \quad (14)$$

where  $E_{\text{p}}^*$  is determined by the masses of the proton, pion and  $\Lambda$ , as in Eq. (2). We take the event average of  $\langle \mathbf{p} \rangle_{\text{ev}}$ ,

$$\langle \mathbf{p} \rangle_{\text{ev}} = \langle \mathbf{p}^* \rangle_{\text{ev}} + \left\langle \frac{\mathbf{p}_{\Lambda}(\mathbf{p}^* \cdot \mathbf{p}_{\Lambda})}{m_{\Lambda}(E_{\Lambda} + m_{\Lambda})} \right\rangle_{\text{ev}}, \quad (15)$$

where we have used  $\langle \mathbf{p}_{\Lambda} \rangle_{\text{ev}} = 0$ .

In order to evaluate the second event average in the right-hand-side of Eq. (15), we make two assumptions: (1)  $\mathbf{p}_{\Lambda}$  and  $\mathbf{p}^*$  are statistically independent, so we have  $\langle \mathbf{p}_{\Lambda}(\mathbf{p}^* \cdot \mathbf{p}_{\Lambda}) \rangle_{\text{ev}} \approx e_i \langle \mathbf{p}_{\Lambda}^i \mathbf{p}_{\Lambda}^j \rangle_{\text{ev}} \langle \mathbf{p}_j^* \rangle_{\text{ev}}$ , where  $\mathbf{p}_{\Lambda} = e_i \mathbf{p}_{\Lambda}^i$  with  $i = x, y, z$ ; and (2)  $\langle \mathbf{p}_{\Lambda}^i \mathbf{p}_{\Lambda}^j \rangle_{\text{ev}} = \langle |\mathbf{p}_{\Lambda}^i|^2 \rangle_{\text{ev}} \delta_{ij}$ . Eq. (15) then becomes

$$\begin{aligned} \langle \hat{\mathbf{p}}_x^* \rangle_{\text{ev}} &\approx \frac{1}{|\mathbf{p}^*|} \left( 1 + \left\langle \frac{|\mathbf{p}_{\Lambda}^x|^2}{(E_{\Lambda} + m_{\Lambda})m_{\Lambda}} \right\rangle_{\text{ev}} \right)^{-1} \langle \mathbf{p}_x \rangle_{\text{ev}}, \\ \langle \hat{\mathbf{p}}_y^* \rangle_{\text{ev}} &\approx \frac{1}{|\mathbf{p}^*|} \left( 1 + \left\langle \frac{|\mathbf{p}_{\Lambda}^y|^2}{(E_{\Lambda} + m_{\Lambda})m_{\Lambda}} \right\rangle_{\text{ev}} \right)^{-1} \langle \mathbf{p}_y \rangle_{\text{ev}}, \\ \langle \hat{\mathbf{p}}_z^* \rangle_{\text{ev}} &\approx \frac{1}{|\mathbf{p}^*|} \left( 1 + \left\langle \frac{|\mathbf{p}_{\Lambda}^z|^2}{(E_{\Lambda} + m_{\Lambda})m_{\Lambda}} \right\rangle_{\text{ev}} \right)^{-1} \langle \mathbf{p}_z \rangle_{\text{ev}}. \end{aligned} \quad (16)$$

We choose a coordinate system as in Fig. 1: the impact parameter vector is along the  $x$ -axis, the global orbital momentum is along the  $y$ -axis, and the beam direction is along the negative  $z$ -axis. In the coordinate system used in the experiment, the beam direction is along the negative  $z$ -axis, and the impact parameter vector (reaction plane) is at an azimuthal angle  $\psi_{\text{RP}}$  relative to the  $x$ -axis. In the new coordinate system, we have  $\mathbf{p}_{\Lambda, \text{p}}^x = |\mathbf{p}_{\Lambda, \text{p}}^T| \cos(\phi_{\Lambda, \text{p}} - \psi_{\text{RP}})$  and  $\mathbf{p}_{\Lambda, \text{p}}^y = |\mathbf{p}_{\Lambda, \text{p}}^T| \sin(\phi_{\Lambda, \text{p}} - \psi_{\text{RP}})$ , where  $\phi_{\Lambda, \text{p}}$  are the azimuthal angles of the  $\Lambda$  hyperon and proton, respectively.

We can further simplify Eq. (16) by using the elliptic flow coefficients. The distribution of  $\mathbf{p}_{\Lambda}$  is not isotropic but satisfies

$$\begin{aligned} \langle |\mathbf{p}_{\Lambda}^x|^2 \rangle_{\text{ev}} &\approx \langle |\mathbf{p}_{\Lambda}^T|^2 \rangle_{\text{ev}} \langle \cos^2(\phi_{\Lambda} - \psi_{\text{RP}}) \rangle_{\text{ev}} \\ &\approx \langle |\mathbf{p}_{\Lambda}^T|^2 \rangle_{\text{ev}} \frac{1}{2} (1 + v_2^{\Lambda}), \\ \langle |\mathbf{p}_{\Lambda}^y|^2 \rangle_{\text{ev}} &\approx \langle |\mathbf{p}_{\Lambda}^T|^2 \rangle_{\text{ev}} \langle \sin^2(\phi_{\Lambda} - \psi_{\text{RP}}) \rangle_{\text{ev}} \\ &\approx \langle |\mathbf{p}_{\Lambda}^T|^2 \rangle_{\text{ev}} \frac{1}{2} (1 - v_2^{\Lambda}), \end{aligned} \quad (17)$$

where  $v_2^{\Lambda}$  is the elliptic flow of the  $\Lambda$  hyperon. Since the global angular momentum is along the  $y$ -axis, we have  $\langle \mathbf{p}_x \rangle_{\text{ev}} = \langle \mathbf{p}_z \rangle_{\text{ev}} = 0$ , and the only non-vanishing component is

$$\begin{aligned} \langle \hat{\mathbf{p}}_y^* \rangle_{\text{ev}} &\approx \frac{1}{|\mathbf{p}^*|} \left( 1 + \left\langle \frac{|\mathbf{p}_{\Lambda}^T|^2 \sin^2(\phi_{\Lambda} - \psi_{\text{RP}})}{(E_{\Lambda} + m_{\Lambda})m_{\Lambda}} \right\rangle_{\text{ev}} \right)^{-1} \\ &\quad \times \langle |\mathbf{p}_T| \sin(\phi_{\text{p}} - \psi_{\text{RP}}) \rangle_{\text{ev}} \\ &\approx \frac{1}{|\mathbf{p}^*|} \left[ 1 + \frac{1}{2} (1 - v_2^{\Lambda}) \left\langle \frac{|\mathbf{p}_{\Lambda}^T|^2}{(E_{\Lambda} + m_{\Lambda})m_{\Lambda}} \right\rangle_{\text{ev}} \right]^{-1} \\ &\quad \times \langle |\mathbf{p}_T| \sin(\phi_{\text{p}} - \psi_{\text{RP}}) \rangle_{\text{ev}} \end{aligned} \quad (18)$$

In the central rapidity region  $|\mathbf{p}_{\Lambda}^z| \ll |\mathbf{p}_{\Lambda}^T|$  and  $|\mathbf{p}_{\Lambda}^T| \approx |\mathbf{p}_{\Lambda}|$ , so that Eq. (18) becomes

$$\begin{aligned} \langle \hat{\mathbf{p}}_y^* \rangle_{\text{ev}} &\approx \frac{1}{|\mathbf{p}^*|} \left[ 1 + \frac{1}{2} (1 - v_2^{\Lambda}) (\langle \gamma_{\Lambda} \rangle_{\text{ev}} - 1) \right]^{-1} \\ &\quad \times \langle |\mathbf{p}_T| \sin(\phi_{\text{p}} - \psi_{\text{RP}}) \rangle_{\text{ev}} \end{aligned} \quad (19)$$

In the non-relativistic limit,  $\gamma_{\Lambda} \approx 1$  and  $|\mathbf{v}_{\Lambda}| \approx 0$ , we obtain

$$\langle \hat{\mathbf{p}}_y^* \rangle_{\text{ev}} \approx \frac{1}{|\mathbf{p}^*|} \langle |\mathbf{p}_T| \sin(\phi_{\text{p}} - \psi_{\text{RP}}) \rangle_{\text{ev}} \quad (20)$$

The difference with respect to the STAR method is that now we are taking the event average using the proton momenta in the lab frame.

Another method is to use the Lorentz transformation of the energy associated with Eq. (14)

$$E_{\text{p}} = \gamma_{\Lambda} E_{\text{p}}^* + \frac{\mathbf{p}^* \cdot \mathbf{p}_{\Lambda}}{m_{\Lambda}} \quad (21)$$

to replace  $(\mathbf{p}^* \cdot \mathbf{p}_{\Lambda})/m_{\Lambda}$  with  $E_{\text{p}} - \gamma_{\Lambda} E_{\text{p}}^*$ . Eq. (14) then becomes

$$\begin{aligned} \mathbf{p} &= \mathbf{p}^* + (E_{\text{p}} - \gamma_{\Lambda} E_{\text{p}}^*) \frac{\mathbf{p}_{\Lambda}}{E_{\Lambda} + m_{\Lambda}} + \frac{E_{\text{p}}^*}{m_{\Lambda}} \mathbf{p}_{\Lambda} \\ &= \mathbf{p}^* + \frac{E_{\text{p}}}{E_{\Lambda} + m_{\Lambda}} \mathbf{p}_{\Lambda} + \frac{E_{\text{p}}^*}{E_{\Lambda} + m_{\Lambda}} \mathbf{p}_{\Lambda}. \end{aligned} \quad (22)$$

Taking the event average and using  $\langle \mathbf{p}_{\Lambda} / (E_{\Lambda} + m_{\Lambda}) \rangle_{\text{ev}} \approx 0$ , we obtain

$$\begin{aligned} \langle \mathbf{p}^* \rangle_{\text{ev}} &= \langle \mathbf{p} \rangle_{\text{ev}} - \left\langle \frac{E_{\Lambda}}{E_{\Lambda} + m_{\Lambda}} E_{\text{p}} \mathbf{v}_{\Lambda} \right\rangle_{\text{ev}} \\ &= m_{\text{p}} \left\langle \gamma_{\text{p}} \left( \mathbf{v}_{\text{p}} - \frac{\gamma_{\Lambda}}{\gamma_{\Lambda} + 1} \mathbf{v}_{\Lambda} \right) \right\rangle_{\text{ev}}, \end{aligned} \quad (23)$$

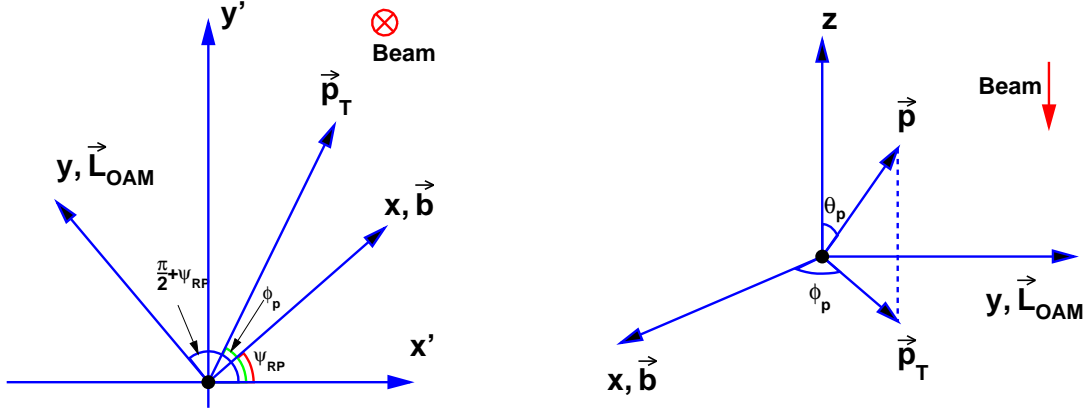


Fig. 1. (color online) In the coordinate system  $(x, y, z)$ , the beam direction is along the negative  $z$ -direction, the impact parameter vector is in the  $x$ -direction, and the orbital angular momentum is in the  $y$ -direction. The direction of the proton momentum can be described by the polar angle  $\theta_p$  and the azimuthal angle  $\phi_p$ . The coordinate system  $(x', y', z')$  is used in experiment. The  $z'$ -axis is just the  $z$ -axis. The azimuthal angle of the impact parameter vector in the  $(x', y', z')$  system is  $\psi_{RP}$ .

where  $\gamma_p$  and  $\gamma_\Lambda$  are Lorentz contraction factors for the proton and  $\Lambda$  hyperon, respectively. The right-hand-side of the above equation involves only momenta in the lab frame. We can project Eq. (23) onto the  $y$ -direction (the direction of the orbital angular momentum) to obtain  $\langle \hat{p}_y^* \rangle_{ev}$ .

With  $\langle \hat{p}_y^* \rangle_{ev}$  given by one of Eqs. (18, 19, 23), we can obtain the global polarization of  $\Lambda$  from Eq. (13). In the next section we compare these methods by simulations.

## 5 Simulation results with UrQMD

The UrQMD model [31, 32] has been used to produce an ensemble of  $\Lambda$  hyperon four-momenta  $(E_\Lambda, \mathbf{p}_\Lambda)$  from Au+Au collisions with an impact parameter of 6 fm and collision energies listed in Table 1. In each event there

$\Lambda$  hyperons using the methods given by Eqs. (8, 11, 18, 23, 19) are shown in Table 1. We see that all proposed methods give equivalent results to the STAR method. Fig. 2 shows the dependence of the simulation results on the rapidity ranges. We conclude that all methods work well for the chosen rapidity ranges, except method Eq. (19) when used in the full rapidity range, or in ranges  $[-1.5, 1.5]$  and  $[-1, 1]$ . This is understandable since Eq. (19) is only valid for central rapidity. When applied in the rapidity range  $[-0.5, 0.5]$ , this method also works well.

## 6 Summary

The method used in the STAR experiment for measurement of the global polarization of  $\Lambda$  hyperons is by event averaging of  $\sin(\phi_p^* - \psi_{RP})$ , where  $\phi_p^*$  and  $\psi_{RP}$  are

are a few  $\Lambda$  hyperons produced. All these hyperons are collected. Each hyperon is allowed to decay into a proton and a pion, whose angular distribution in the  $\Lambda$  rest frame is given by

$$\frac{dN}{d\Omega^*} = \frac{1}{4\pi} \left( 1 + \alpha_H \mathcal{P}_\Lambda \frac{\mathbf{n}^* \cdot \mathbf{p}^*}{|\mathbf{p}^*|} \right), \quad (24)$$

where  $\mathcal{P}_\Lambda$  denotes the  $\Lambda$  polarization. By taking a specific value of  $\mathcal{P}_\Lambda$ , we sample proton momenta in  $\Lambda$  rest frames. For each  $\Lambda$  hyperon, the proton momentum in its rest frame is then boosted back to the lab frame. In this way we create an ensemble of proton momenta in the lab frame. With the ensemble of momenta for protons and  $\Lambda$  hyperons, we obtain  $\langle \hat{p}_y^* \rangle_{ev}$ . Here we choose the direction of the global angular momentum along the  $y$ -direction. Finally, we obtain  $\mathcal{P}_\Lambda$  from Eq. (13). Simulation results for the global polarization of

the azimuthal angles of the proton momentum in the  $\Lambda$  rest frame and of the reaction plane, respectively. We propose several alternative methods for measurement of the  $\Lambda$  global polarization. Based on the Lorentz transformation of momenta, we express the global polarization in terms of momenta of protons and  $\Lambda$  hyperons in the lab frame, and the event average is then taken of relevant quantities in this frame. To test these methods, we used the UrQMD model to produce an ensemble of  $\Lambda$  hyperon momenta and then sampled the angular distribution of protons and pions following the weak decay of  $\Lambda$  hyperons. By taking event averages of relevant quantities as function of momenta of protons and  $\Lambda$  hyperons in the lab frame, we determined the global polarization. The simulations showed that all proposed methods work equally well as the STAR method.

Table 1. Simulation results for the global polarization of  $\Lambda$  hyperons. We set  $\mathcal{P}_\Lambda = 1/3$ , i.e. the  $\Lambda$  hyperons are completely polarized. By analyzing the momentum distribution of daughter protons in the lab frame, we determine the  $\Lambda$  polarization. The results of five methods are presented: methods 1 and 2, Eqs. (8,11) are used in the STAR experiment [21]; methods 3–5, given by Eqs. (18, 23, 19) are proposed in this paper. The number of events collected are  $4 \times 10^4$  at 200 GeV and  $2.5 \times 10^4$  at other energies. The results of method 1-4 are from events in the full rapidity range, while those of method 5 are in the rapidity range  $[-0.5, 0.5]$ .

energy/ GeV	method 1 Eq. (8)	method 2 Eq. (11)	method 3 Eq. (18)	method 4 Eq. (23)	method 5 Eq. (19)	number of $\Lambda$ s (full rapidity)
200	0.33581	0.335851	0.3324	0.33014	0.308495	1304795
180	0.330877	0.33141	0.326565	0.329057	0.306966	927717
140	0.338745	0.337673	0.338942	0.335862	0.351934	892533
120	0.333962	0.333688	0.329696	0.334152	0.318965	995522
100	0.336686	0.334685	0.34669	0.34522	0.360992	971596
62.4	0.331964	0.33118	0.324133	0.333466	0.353216	918787
40	0.330536	0.330302	0.332092	0.331782	0.323459	795837
39	0.337252	0.337516	0.332983	0.331683	0.312195	847367
19.6	0.328531	0.328434	0.339587	0.328939	0.31276	707868
7.7	0.341257	0.3417	0.364069	0.34862	0.302301	434697

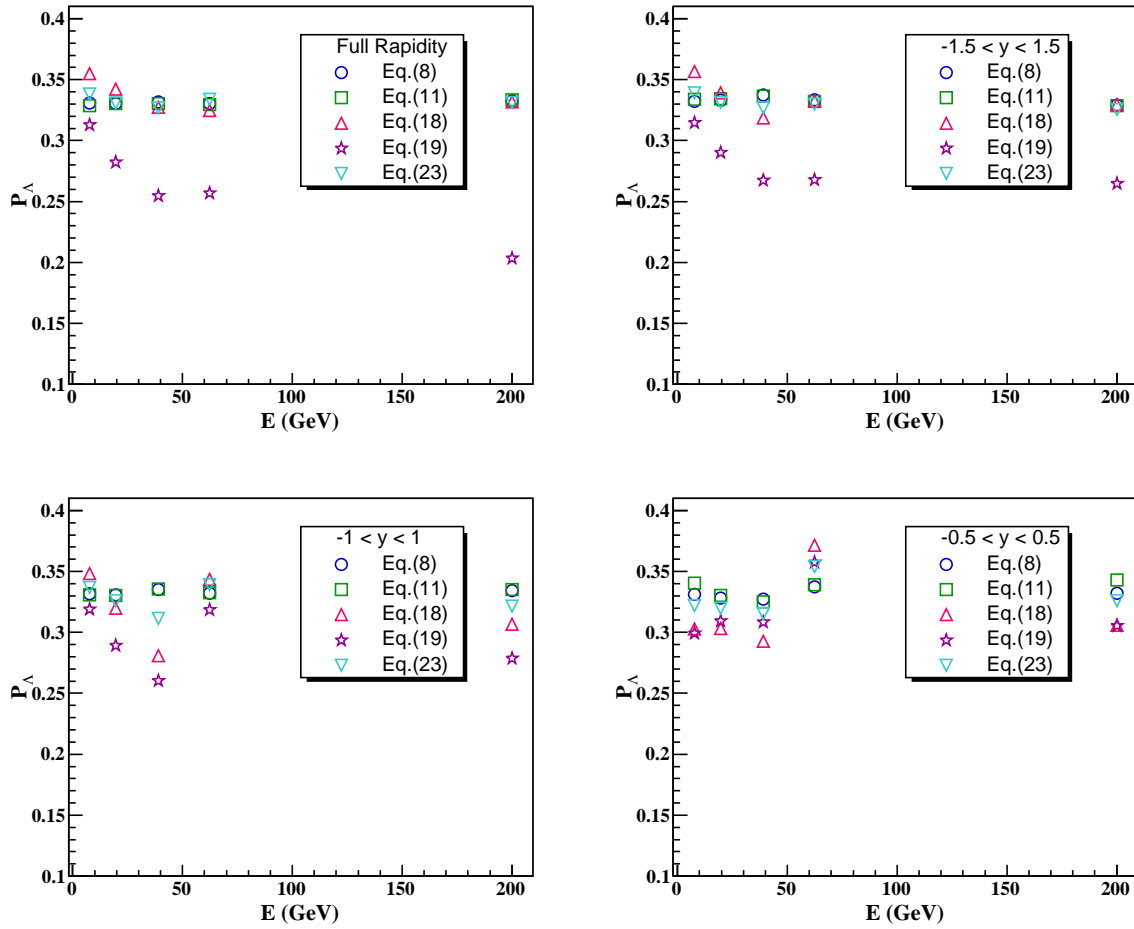


Fig. 2. (color online) The dependence of simulation results on rapidity ranges for the global polarization of the  $\Lambda$  hyperon. The same parameters and number of events are used as in Table 1.

## References

- 1 S. Barnett, *Rev. Mod. Rev.*, **7**: 129 (1935)
- 2 A. Einstein and W. de Haas, *Deutsche Physikalische Gesellschaft, Verhandlungen*, **17**: 152 (1915)
- 3 Z.-T. Liang and X.-N. Wang, *Phys. Rev. Lett.*, **94**: 102301 (2005); *Phys. Rev. Lett.*, **96**: 039901 (2006), [nucl-th/0410079](#)
- 4 Z.-T. Liang and X.-N. Wang, *Phys. Lett. B*, **629**: 20 (2005), [nucl-th/0411101](#)
- 5 S. A. Voloshin (2004), [nucl-th/0410089](#)
- 6 B. Betz, M. Gyulassy, and G. Torrieri, *Phys. Rev. C*, **76**: 044901 (2007), [arXiv:0708.0035](#)
- 7 F. Becattini, F. Piccinini, and J. Rizzo, *Phys. Rev. C*, **77**: 024906 (2008), [arXiv:0711.1253](#)
- 8 J.-H. Gao, S.-W. Chen, W.-t. Deng, Z.-T. Liang, Q. Wang, and X.-N. Wang, *Phys. Rev. C*, **77**: 044902 (2008), [arXiv:0710.2943](#)
- 9 S.-w. Chen, J. Deng, J.-h. Gao, and Q. Wang, *Front. Phys. China*, **4**: 509 (2009), [arXiv:0801.2296](#)
- 10 F. Becattini and L. Tinti, *Annals Phys.*, **325**: 1566 (2010), [arXiv:0911.0864](#)
- 11 F. Becattini, *Phys. Rev. Lett.*, **108**: 244502 (2012), [arXiv:1201.5278](#)
- 12 F. Becattini, V. Chandra, L. Del Zanna, and E. Grossi, *Annals Phys.*, **338**: 32 (2013), [arXiv:1303.3431](#)
- 13 F. Becattini and E. Grossi, *Phys. Rev. D*, **92**: 045037 (2015), [arXiv:1505.07760](#)
- 14 J.-H. Gao, Z.-T. Liang, S. Pu, Q. Wang, and X.-N. Wang, *Phys. Rev. Lett.*, **109**: 232301 (2012), [arXiv:1203.0725](#)
- 15 J.-W. Chen, S. Pu, Q. Wang, and X.-N. Wang, *Phys. Rev. Lett.*, **110**: 262301 (2013), [arXiv:1210.8312](#)
- 16 R.-h. Fang, L.-g. Pang, Q. Wang, and X.-n. Wang, *Phys. Rev. C*, **94**: 024904 (2016), [arXiv:1604.04036](#)
- 17 R.-h. Fang, J.-y. Pang, Q. Wang, and X.-n. Wang, *Phys. Rev. D*, **95**: 014032 (2017), [arXiv:1611.04670](#)
- 18 Q. Wang, in *26th International Conference on Ultra-relativistic Nucleus-Nucleus Collisions (Quark Matter 2017) Chicago, Illinois, USA, February 6-11, 2017* (2017), [arXiv:1704.04022](#), <http://inspirehep.net/record/1591567/files/arXiv:1704.04022.pdf>.
- 19 O. E. Overseth and R. F. Roth, *Phys. Rev. Lett.*, **19**: 391 (1967)
- 20 L. Adamczyk et al. (STAR), *Nature*, **548**: 62 (2017), [arXiv:1701.06657](#)
- 21 B. I. Abelev et al. (STAR), *Phys. Rev. C*, **76**: 024915 (2007), [arXiv:0705.1691](#)
- 22 L. P. Csernai, V. K. Magas, and D. J. Wang, *Phys. Rev. C*, **87**: 034906 (2013), [1302.5310](#).
- 23 L. P. Csernai, D. J. Wang, M. Bleicher, and H. Stoecker, *Phys. Rev. C*, **90**: 021904 (2014)
- 24 L.-G. Pang, H. Petersen, Q. Wang, and X.-N. Wang, *Phys. Rev. Lett.*, **117**: 192301 (2016), [arXiv:1605.04024](#)
- 25 Y. Jiang, Z.-W. Lin, and J. Liao, *Phys. Rev. C*, **94**: 044910 (2016), [arXiv:1602.06580](#)
- 26 W.-T. Deng and X.-G. Huang, *Phys. Rev.* **93**: 064907 (2016), [arXiv:1603.06117](#)
- 27 I. Karpenko and F. Becattini, *Eur. Phys. J. C*, **77**: 213 (2017), [arXiv:1610.04717](#)
- 28 Y. Xie, D. Wang, and L. P. Csernai, *Phys. Rev. C*, **95**: 031901 (2017), [arXiv:1703.03770](#)
- 29 H. Li, L.-G. Pang, Q. Wang, and X.-L. Xia (2017), [arXiv:1704.01507](#)
- 30 Y. Sun and C. M. Ko, *Phys. Rev. C*, **96**: 024906 (2017), [arXiv:1706.09467](#)
- 31 S. A. Bass et al., *Prog. Part. Nucl. Phys.*, **41**: 255 (1998), [*Prog. Part. Nucl. Phys.*, **41**: 225 (1998)], [nucl-th/9803035](#)
- 32 H. Petersen, J. Steinheimer, G. Burau, M. Bleicher, and H. Stoecker, *Phys. Rev. C*, **78**: 044901 (2008), [arXiv:0806.1695](#)